Журнал нано- та електронної фізики
Том **16** № 4, 04034(6cc) (2024)

Journal of Nano- and Electronic Physics
Vol. **16** No 4, 04034(6pp) (2024)

OPEN ACCESS

REGULAR ARTICLE

Some Kinetic Peculiarities of Formation of High-Entropy Oxide $Co_{0.2}Ni_{0.2}Cu_{0.2}Mg_{0.2}Zn_{0.2}O$

M.P. Semenko*

Taras Shevchenko National University of Kyiv, 01601 Kyiv, Ukraine

(Received 14 May 2024; revised manuscript received 21 August 2024; published online 27 August 2024)

The kinetics of the formation of high-entropy oxide $Co_{0.2}Ni_{0.2}Cu_{0.2}Mg_{0.2}Zn_{0.2}O$ from the initial powder mixture of oxide components was studied for the first time by X-ray diffraction. It has been shown that the dissolution of CuO oxide at the last stage of the formation of this oxide can be described using the Johnson-Mell-Avrami model. Based on the analysis of the results obtained under isothermal conditions, the kinetic parameters of the process were estimated. The value of the Avrami index indicates that the formation process at this stage occurs without nucleation by the diffusion mechanism with a change in the nature of diffusion as the composition approaches the nominal one.

Keywords: High-entropy oxide, Kinetic parameter, X-ray diffraction.

DOI: 10.21272/jnep.16(4).04034 PACS numbers: 81.05.Zx, 05.70.Ce, 61.43. – j

1. INTRODUCTION

High-entropy oxides (HEOs) are a type of material in which the effect of entropic stabilization of the crystal structure is realized, first discovered in the so-called high-entropy alloys (HEAs) in 2004 [1]. It is the uniqueness of the properties of HEAs (see review [2]) that gave rise to the search for the high-entropy effect in other types of materials. Today, high-entropy stabilized structures have been found in oxides, carbides, nitrides, borides and sulfides.

Among these materials, HEOs have perhaps the largest representation, which is due to the wide variety of conventional oxide structures. Oxide of composition $Co_{0.2}Ni_{0.2}Cu_{0.2}Mg_{0.2}Zn_{0.2}O$ with a rock salt structure (R-HEO) is the first synthesized HEO [3]. In HEO, the high configurational entropy applies only to the cationic subsystem and does not affect the anionic subsystem (oxygen). However, as in HEAs, the cation content must be the same to realise the maximum effect of the configurational entropy. After the synthesis of HEOs with the structure of rock salt, HEOs with other types of crystal structures, such as fluorites, bixbits, perovskites, and others, were obtained (a review of such systems can be found, for example, in [4,5]).

The HEO of the composition $Co_{0.2}Ni_{0.2}Cu_{0.2}Mg_{0.2}Zn_{0.2}O$ (hereinafter referred to as R-HEO) has its advantages as the first and most studied material and the material with a fairly simple crystal cell of the rock salt type (space group *Fm*-3*m*). Already in the first declarative work [3] on the synthesis of R-HEO, much attention was paid to the study of the conditions for the synthesis of this material and the role of small variations in composition on these conditions. As it was shown in [6], the local crystal structure in R-HEO is quite sensitive to the copper content and thermal prehistory of the samples. The study of the sequence of transformations of the mixture of oxides with increasing synthesis temperature allowed to establish that the formation of R-HEO correlates with the energy of vacancy formation in oxides [7]. Since CuO and ZnO oxides have a structure different from that of rock salt, they need to pass the energy barrier associated with a change in the crystal structure and these oxides dissolve in the R-HEO structure at the final stage of synthesis. The latter is the dissolution of CuO oxide, which is in full agreement with the results of [3]. The energy of the formation process, which actually determines the temperature of synthesis and the stability of HEO, is related not only to the entropic contribution, but also to the energy required for the transformation of wurtzite ZnO and tenorite CuO to the FCC of the structural rock salt. Although the formation of the R-phase revealed an endothermic maximum on the DSC during the transition from the multiphase to the single-phase state [3], the kinetics of the formation of R-HEO, as well as other HEOs, has not been studied directly to date. Therefore, the aim of this work was to investigate the kinetics of formation of the $Co_{0.2}Ni_{0.2}Cu_{0.2}Mg_{0.2}Zn_{0.2}O$ HEO.

2. EXPERIMENTAL DETAILS

As a starting material for the study, a mixture of CoO, CuO, MgO, NiO, and ZnO oxides with a purity of at least 99.99 %, taken in the appropriate proportion corresponding to the stoichiometry of cations in R-HEO, was used. This mixture was thoroughly mixed and manually ground. After that, this mixture was loaded into a heated furnace, first to a temperature of $T_1 = 920$ °C and then to a temperature of $T_2 = 985$ °C. The first temperature is slightly higher than the temperature of the beginning of R-HEO formation (850-900 °C [3]) and was chosen to slow down the formation of R-HEO to study the kinetics.

* Correspondence e-mail: smp@univ.kiev.ua

Cite this article as: M.P. Semenko, *J. Nano- Electron. Phys.* 16 No 4, 04034 (2024) https://doi.org/10.21272/jnep.16(4).04034

The first annealing was carried out for 6 hours. After each annealing period, the powder was air quenched and ground. A small amount of this powder was used for X-ray studies, and the rest was annealed again for a certain period. It was assumed that the annealing time was equal to the sum of the annealing times for the previous periods. An increase in the annealing temperature to 985 °C was associated with a slowdown in the transformation processes, which required rather long annealing times.

Powder diffraction patterns were obtained at room temperature on an automated X-ray diffractometer DRON-4-07 using $Cu_{\alpha 1 \alpha 2}$ radiation.

The resulting diffraction patterns were refined using FULLPROF software [8]. First, the parameters of the FCC structure were refined. To do this, the intervals where the peaks of CuO are located were excluded from the calculations , and then, fixing these parameters, the parameters of CuO and their volume contents were calculated. The R-HEO structure was refined using the structure file for NiO, which was modified in accordance with the composition of the cationic group of HEO. The same, for comparison, were refined using the Le Baille method [9], which is also implemented in FULLPROF software.

3. RESULTS

3.1 X-ray Diffraction Results

The results of X-ray diffraction from R-HEO powder at different stages of heat treatment are shown in Fig. 1. Each of the X-ray diffraction pattern is presented after subtraction of the background and normalisation to the maximum intensity of the diffraction maximum (200), I_{max200}.

As can be seen, annealing at T_1 for 6 hours (sample R1) leads to the formation of a two-phase structure containing phases of HEO with the structure of rock salt and tenorite CuO. In other words, these studies consider the last stage of formation of the stoichiometric structure of R-HEO. As the annealing time increases, the intensity of the CuO diffraction peaks decreases, but this phase does not disappear even after annealing at this temperature for 20 hours.

Fig. 2 shows the change with annealing time, t, of the relative intensity of the diffraction maxima of CuO oxide and R-HEO, $\eta_{(hkl)} = I_T/I_{(hkl)}$, where I_T is the intensity (area under the peak) of the CuO maximum and $I_{(hkl)}$ is the intensity of the diffraction maximum (hkl) of R-HEO. The most intense diffraction maximum, which is a superposition of the (111) and (200) maxima, was chosen as the tenorite maximum, and both the (111) and (200) maxima were used as the R-HEO diffraction maximum. In this case, the intensities were calculated as the areas under the maxima (without taking into account the background and peak shape). As the relative intensities of the (111) and (200) R-HEO diffraction maxima, $I_{(111)}/I_{(200)}$, for all anneals are within (60 ± 4) %, then it can be assumed that the dependence $\eta_{(hkl)}$ on t is due to the decrease in the amount of CuO. This is evidenced by the superposition of both dependences when normalized to the values obtained for R1: the dependences $x = \eta(t)/\eta(\mathrm{R1})$ on t for different (hkl), are practically the same.

As can be seen from Fig. 2, the rate of change of η with t increases with an increase in the annealing temperature T to 985 °C, which indicates an increase in the rate of CuO dissolution in R-HEO. Annealing at this temperature for 9.5 hours (from 20 to 29.5 hours of total annealing) leads to the formation of an almost single-phase structure of R-HEO (only the remnants of the most intense CuO maxima are observed in Fig. 1). Further annealing at 1000 °C leads to the formation of a single-phase R-HEO structure, but, most likely, a single-phase structure should also form at T_2, but at longer annealing times.

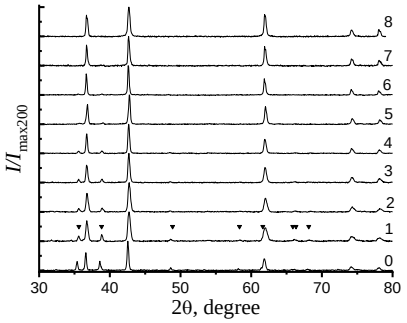

Fig. 1 – X-ray diffraction patterns of the powder of composition R-HEO after successive annealing for 6 (1), 10 (2), 14 (3), 20 (4), 22.5 (5), 25 (6), 29.5 (7) and 45 (8) hours. The anneals (1)-(4) were performed at T = 920 °C, (5)-(7) - at T = 985 °C, (8) - at T = 1000 °C. (0) - X-ray diffraction pattern from a mechanical mixture of CuO and HEO of the composition $Co_{0.25}Ni_{0.25}Zn_{0.25}Mg_{0.25}O$ of the total nominal composition. Triangles correspond to the positions of the main diffraction maxima of tenorite CuO

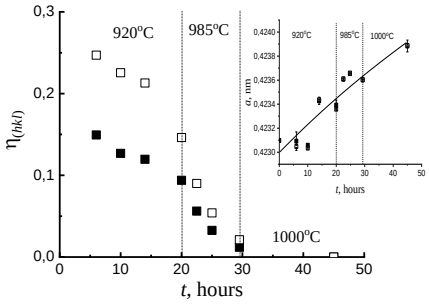

Fig. 2 – Dependence of the relative intensities (areas under the peaks), $\eta_{(hkl)}$, of the diffraction maximum of CuO tenorite with the maximum intensity (superposition of (111) and (200)), to the diffraction maxima (111) (dark squares) and (200) (light squares) of R-HEO on the annealing time, t, at the temperatures indicated in the figure. Inset: dependence of the cell parameter, a, of the FCC R-HEO on the annealing time, t: dark squares are obtained by the Rietveld method, light squares – by the LeBaille method

Therefore, the relative intensities of the diffraction maxima of tenorite and FCC R-HEO presented in Fig. 2 are mainly determined by the tenorite content. This is only possible if the structure of R-HEO remains unchanged. However, it is quite clear that the copper cations of the part of CuO that has disintegrated are dissolved in R-HEO. As a result, a change in the structure parameters of the rock salt should be observed, primarily due to changes in the cell parameters and form factors that determine the intensity of diffraction maxima.

The change of structure of the R-HEO due to copper dissolution is manifested in the dependence of the cell parameter of the R-HEO, a, on the annealing time, t. This dependence is shown in the inset of Fig. 2. As can be seen, the parameter a increases from about 0.4230 nm to 0.4239

nm as the annealing time increases. The dependences shown in Fig. 2 are plotted for the parameter a determined by both the Rietveld method (black squares) and the Le Baille method (white squares). Almost the same dependences were obtained using the graphical method, when the positions of each of the R-HEO diffraction maxima were determined separately, and the parameter a was determined by graphical approximation (these dependences are not shown in the graph).

It can be assumed that the dependence of a on t is a consequence of Wegart's law, when the lattice parameter of solid solutions is determined by the average radii of the dissolved components, $\langle R_K \rangle$. In this case, we are talking about the dissolution of copper cations in the R-HEO lattice. In the case of a four-component composition without Cu^{2+} ion, $\langle R_K \rangle = 0.700$ nm, and for a five-component composition, $\langle R_K \rangle = 0.706$ nm (the estimate was made taking into account the R_K given in [10]). Such changes in the average value are 0.9%, and the maximum changes in a (between the maximum and minimum values of a in Fig. 3) are less than 0.3%, which should be considered as a consequence of partial dissolution of copper in sample R1.

3.2 Quantitative Phase Analysis

The influence of the cationic composition on the results of quantitative phase analysis was tested for sample R1. For this purpose, the experimental diagram was analysed by the Rietveld method for two limiting compositions: a five-component oxide with the nominal composition $Co_{0.2}Ni_{0.2}Zn_{0.2}Mg_{0.2}Cu_{0.2}O$ and a four-component oxide with the composition $Co_{0.25}Ni_{0.25}Zn_{0.25}Mg_{0.25}O$. The composition of the cationic group changed during the calculations.

In the first case, the volume content f_T of tenorite was found to be f_T = 14(2) % with unit cell volumes $v_R = 75.747(24)\cdot10^{-3}$ nm^3 and $v_T = 80.688(51)\cdot10^{-3}$ nm^3 for R-HEO and tenorite, respectively. In the second case, the volume content f of tenorite was found to be f_T = 13(2) % CuO with cell volumes v_R = 75.749(24)·10 $^{-3}$ nm^3 and v_T = 80.694(54)·10 $^{-3}$ nm^3. From these results, it follows that the scattering ability of the R-HEO cationic system (atomic scattering factor) has a rather weak effect on the results of quantitative analysis. Varying the composition of the cationic group leads to a difference in the volume content of copper oxide of 1 %, which is less than the errors in the determination of the composition.

Since five $Co_{0.2}Ni_{0.2}Zn_{0.2}Mg_{0.2}Cu_{0.2}O$ lattices can form four $Co_{0.25}Ni_{0.25}Zn_{0.25}Mg_{0.25}O$ lattices and one CuO lattice, the volume content of tenorite in such a mixture is $f_T = v_T/(v_T + 4v_R)$. With v_R and v_T values obtained by the Rietveld method, we have f_T = 21 %. This value is almost twice as large as that obtained in the two limit cases. Thus, the sample annealed for t = 6 h at T_1 has an R-HEO lattice with partially dissolved copper.

The correctness of this assessment and the results of the phase analysis are confirmed by the results of diffraction studies of the mechanical mixture of tenorite and the $Co_{0.25}Ni_{0.25}Zn_{0.25}Mg_{0.25}O$ HEO synthesised for this purpose, taken in proportions that corresponded to the composition $Co_{0.2}Ni_{0.2}Zn_{0.2}Mg_{0.2}Cu_{0.2}O$. The diffraction pattern for such a mixture is shown in Fig. 1 (curve (0)). As a result of the approximation, it was obtained that the volume content of tenorite in this mixture is 23.8(1.5) %, which, even taking into account only the calculation errors, is in good agreement with the estimated values (21 %).

In principle, the Rietveld method makes it possible to refine the concentrations of the relevant constituents (through employment factors). However, since the number of cationic constituents is quite large, their scattering factors do not change significantly, and the concentrations of such constituents are interrelated [3], such a refinement is practically impossible for HEO and will either lead to physically erroneous results or give a general discrepancy when refining the parameters. Therefore, further phase analysis is carried out using the results obtained for the nominal cationic composition. Since the copper concentration in R-HEO increases with the annealing time, it is expected that the additional error due to the uncertainty in the cationic composition will decrease with the annealing time. Such calculations of the volume content of tenorite f_T as a function of annealing time t are shown in Fig. 3.

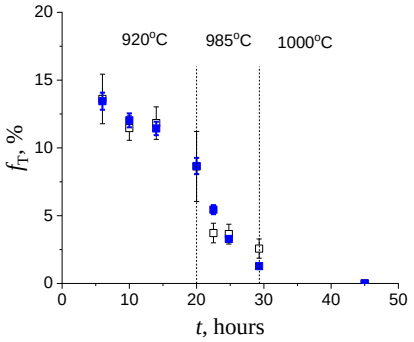

Fig. 3 – Dependence of the fraction of tenorite f_T on the annealing time t (white circles – content determined by the Rietveld method, blue squares – calculations based on the intensity of diffraction maxima)

3.3 The Kinetics of the Transformation Process

The obtained dependence of the tenorite content on the annealing time makes it possible to perform a kinetic analysis of the process occurring at the final stage of R-HEO formation and to estimate the kinetic parameters.

Any kinetic analysis of thermoanalytical data starts from the general expression of the reaction rate of the transformation process [11, 12]:

$$\frac{d\alpha}{dt} = kg(\alpha), \qquad (1)$$

where α is the degree of transformation, $k = k(T) = k_0\exp[-E/(RT)]$, k_0 is the preexponential factor, E is the activation energy, T is the temperature and R is the gas constant. The function $g(\alpha)$ is determined by the kinetic model of the process. The most frequently cited kinetic models are summarized in [11].

Thus, if the dependence of the degree of transformation of one phase into another with time is known, then the kinetic parameters can be found using equation (1) with a known function $g(\alpha)$. In our case, the degree of transformation can be defined as the fraction of the volume content of CuO that has been transformed in the mixture during annealing at time t. If we assume that f_T at $t = 0$ is 23.8 % (a value obtained from diffraction data for the mixture), then α is quite simple: $\alpha = 1 - f_T/23.8$.

In isothermal transformation conditions, the use of the function $g(\alpha)$ in the Johnson-Mell-Avrami (JMA) model [11], allows us to present the dependence of the transformation degree α on time in the form [11]:

$$\alpha(t) = 1 - \exp[-(kt)^n]), \quad (2)$$

where n is a parameter determined in general by the nucleation and growth mechanisms (Avrami parameter). If we represent Eq.(2) in the form of:

$$\ln(-\ln(1-\alpha)) = n\ln k_0 - nE/RT + n\ln t, \quad (3)$$

then it is possible to determine the n and E.

The dependence of ln(– ln(1 – α)) on ln$t$, plotted according to the results presented in Fig. 3, is shown in Fig. 4. As can be seen, the accuracy of determining the values of ln(– ln(1 – α)) calculated taking into account the values of f_T and Δf_T for annealing at T_2 is relatively small, which is due to the small values of f_T. Quite obviously, this is reflected in the accuracy of the parameters of the linear approximation $y = a + bx$ according to Eq.(3). The corresponding values of a_i and b_i for both annealing temperatures are shown in the Table 1. Moreover, the linear approximation for the annealing temperature T_1 was performed without taking into account the data for the last annealing at this temperature (the reasons for this will be discussed below).

The accuracy of CuO determination, especially at low f_T content, can be improved by using the relative intensities $\eta_{(hkl)}$ discussed before. This is due to the fact that the accuracy of f_T determination in the Rietveld method will be determined not only by various model parameters, but also by the intensities of all diffraction maxima for a given angular interval. At low CuO content, weak diffraction maxima are practically not observed, which is reflected in the calculated parameters and concentrations, since the Rietveld method works not with individual maxima but with the totality of all diffraction maxima. Consider how f_T can be determined from the values of $\eta_{(hkl)}$.

The value of $\eta_{(hkl)}$ was defined as $\eta_{(hkl)} = I_T/I_{(hkl)}$. Since the absolute intensity of any diffraction maximum of the i-th phase can be written in a simplified form as follows:

$$I_i = C \cdot f_i \cdot \Omega_i, , \quad (4)$$

where C is a coefficient determined by the shooting conditions (the same for all phases of a given sample), f_i is the volume content of the i-th phase), Ω_i is the specific scattering capacity of a given diffraction maximum (takes into account various factors).

Taking into account Eq. (4), neglecting the difference in absorption coefficients, we can write:

$$\eta_{(hkl)} = \frac{f_T}{1-f_T} \cdot \frac{\Omega_T}{\Omega_{(hkl)}} = \frac{f_T}{1-f_T} \cdot K_{(hkl)} \cdot \quad (5)$$

If the f_T value of at least one of the points in the $\eta_{(hkl)}$ *vs.* t dependencies in Fig. 2 is known, it is quite easy to convert these dependencies into the f_T *vs.* t dependency. For the conversion, we used the Rietveld method data for the first three points in Fig. 2, which allowed us to obtain an array of six concentrations for each t value (two dependencies and three conversion factors). As can be seen from Fig. 3, the accuracy of the f_T values improves for all anneals, the f_T values for anneals at T_1 are almost the same as those obtained by the Rietveld method, but the values after anneals at T_2 change significantly. The dependences of ln(– ln(1 – α)) on ln$t$ recalculated from these f_T values are shown in Fig. 4. A significant change in the slope of the data line after annealing at T_2 is characteristic, but the new data fall within the range of acceptable values of the previous data. The parameters of the linear approximation of the calculated data are listed in Table 1.

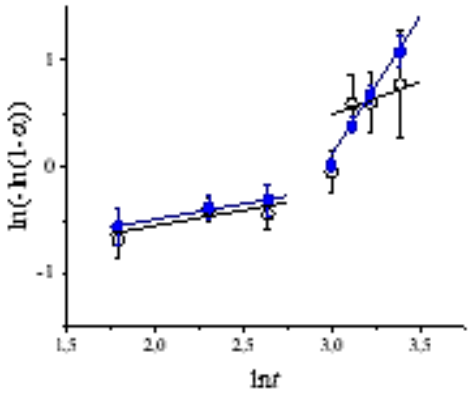

Fig. 4 – Dependence of ln(– ln(1 – α)) on ln$t$ (white circles – content determined by the Rietveld method, blue squares – calculations based on the intensity of diffraction maxima).

The parameters a_i and b_i of the linear approximation for two temperatures T_1 and T_2 allow us to estimate the kinetic parameters n and E. From Eq.(3) it follows that $n_i = b_i$, and the value of E can be estimated only if E and k_0 are independent of T. The values of E obtained in this way for both pairs of values of a_i and b_i are given in the Table.

However, even if E is independent of temperature, questions arise about the validity of the linearity of the dependence of ln(– ln(1 – α)) on ln$t$ if t is the annealing time. In particular, quite often, transformations are characterised by a certain time τ of delay in this transformation (the so-called incubation period [11, 12]), and in our case, there is also uncertainty about the time required to form the initial R-HEO structure from a mixture of oxides. The second question is related to the validity of Eq.(3) for the temperature T_2, since the process at this temperature was not considered from the initial moment, but is a continuation of the synthesis after the temperature T_1. However, since the composition of R-HEO is constantly changing during this synthesis, the decomposition kinetics of CuO can be considered with respect to any initial time t_i. Thus, it can be assumed that Eq.(2) will be valid if t is replaced by $\tau = (t - t_i)$. In this case, the CuO content, $f_T(t_i)$, will be the initial content, and $\alpha = 1 - f_T(\tau)/f_T(t_i)$, where $f_T(\tau)$ is the CuO content at the time that determines τ.

The dependences of ln(– ln(1 – α)) on lnτ obtained for different values of t_i are shown in Fig. 5. Dependence 0 ($t_0 = 0$) in this figure is the dependence of ln(– ln(1 – α)) on ln$t$ shown in Fig. 5, in which α was determined by the intensities of the diffraction maxima. If $t_1 = 6$ h, then this dependence falls lower, but the line that can be drawn through the first two points practically does not change its slope compared to the initial dependence of '0'. Using other values as t_i leads to a change in the character of the dependence. The state of the sample after annealing $t_4 = 20$ h is

Table 1 – The parameters of the linear approximation a and b of the dependences $\ln(-\ln(1-\alpha))$ *vs.* lnt for different temperatures T at different times of the incubation period t_i and the kinetic parameters n and E calculated from these values: 1 – from the data obtained by the Rietveld method, 2 and 3 – from the intensity of the diffraction maximum

N	T, K	t_i, h	a	$b = n$	E, *kJ/mole*
1	1193	0	– 1.13(57)	0.29(24)	340(90)
	1258	0	– 1.34(1.03)	0.61(32)	
2	1193	0	– 1.07(11)	0.29(04)	148(30)
	1258	0	– 7.62(46)	2.58(15)	
3	1193	6	– 2.96	0.55(10)	750(90)
	1258	20	– 1.74	1.06(20)	

the 'initial' state before annealing at T_2. Using the data for this point and the next one after it ($t_5 = 22.5$ h) 'straightens' the dependence $\ln(-\ln(1-\alpha))$ on ln$t$, and the two possible dependences that can be constructed for T_2 are almost identical.

The linear approximation coefficients for the initial interval of dependence (1) and for dependence (4) are given in Table. The same Table 1 shows the calculated values of the parameters n and E.

4. DISCUSSION

Although the statistical accuracy of the results is relatively low (both in terms of temperature and the number of experimental points), the data obtained allow us to make certain conclusions.

Expression (2) is obtained by integrating (1) for the known function g(α) only if the values of n and E are constant for a given temperature T. In our case, it should be assumed that the Avrami index n primarily depends on temperature, which is often found in various types of transformations [13]. It is possible that, in addition, there is a dependence on the concentration of copper dissolved in the HEO. The reason for this is the deviation of the experimental value for the last annealing at T_1 from the time dependence of the previous annealing, but these data are quite good as a starting value for the experimental values obtained during annealing at T_2. This gives reason to assume the presence of some critical value α (or f_T), at which the mechanism of dissolution of Cu cations in the FCC cell of R-HEO changes.

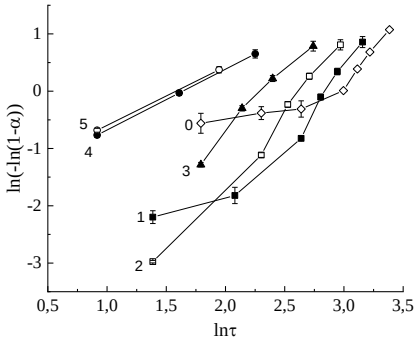

Fig. 5 – Dependences of $\ln(-\ln(1-\alpha))$ on $\ln\tau$ obtained for different $t_i = 0$ (0), 6 (1), 10 (2), 14 (3), 20 (4) and 22.5 (5) hours

The value of the n parameter is defined as [12]:

$$n = d/m + a, \quad (3)$$

where d is the number of directions along which the crystal grows, $m = 1$ in the case of interface-controlled growth, $m = 2$ in the case of diffusion-controlled growth, $a = 0$ at zero or constant nucleation, $a = 1$ at continuous nucleation, $a \geq 1$ at mixed nucleation.

Thus, the values obtained under the assumption that the kinetics is valid for any initial value of time t_i (data 3 in Table) for T_1 are in good agreement for zero nucleation rate ($a = 0$) with one-dimensional ($d = 1$) diffusion ($m = 2$) growth of the new phase. At the same time, the data obtained at T_2 at zero nucleation rate can be interpreted in two ways: as two-dimensional growth ($d = 2$) with diffusion-controlled growth ($m = 2$), or as one-dimensional growth ($d = 1$) with interface-controlled growth ($m = 1$). This change in mechanism may be due to the diffusion measurement of component concentrations when the maximum entropic effect is achieved.

The activation energy obtained in the studies for data 3 in the Table 1 is quite significant. It was calculated under the assumption that the activation energy is constant at all stages of the synthesis. However, given the increasing role of the entropic contribution as CuO decomposes and the Cu^{2+} concentration approaches the equicatation value, this assumption is valid if the entropic changes in energy are small, which is, in principle, true for the final stage of synthesis. It is also noteworthy that the activation energy is several times higher than the energy of transformation of CuO from monoclinic to FCC lattice (~ 22 kJ/mol), which, according to [3], will determine the peculiarities of the formation of HEO at the last stages of synthesis. However, this assumption does not take into account the fact that the formation of HEOs of nominal composition requires not only the transformation of one structure into another, but also the diffusion 'equalisation' of concentrations to achieve the maximum entropic effect. Although the effect of sluggish diffusion has been established only for HEAs, it can be expected in HEOs (unfortunately, there is no information on this). This effect can lead to a significant increase in the activation energy during the synthesis process.

5. CONCLUSIONS

Thus, the study is practically the first study of the kinetic features of the synthesis of HEOs. The results of the study of the synthesis of HEO of the general composition $Co_{0.2}Ni_{0.2}Zn_{0.2}Mg_{0.2}Cu_{0.2}O$ from the initial oxide powders showed the possibility of applying kinetic analysis using the classical approach to process experimental data, in particular, using the Johnson-Mell-Avrami equation. Based on this analysis, it was found that the formation of the oxide at the last stage of CuO dissolution occurs by the diffusion mechanism without the formation of new phase nuclei. It was found that there is a change in the nature of diffusion from one-dimensional to two-dimensional as the cation content approaches the nominal composition. The obtained value of the activation energy of the process significantly exceeds the value of the energy of transformation of CuO from monoclinic to FCC lattice, which can be considered as a consequence of diffusion 'levelling' of concentrations.

ACKNOWLEDGEMENTS

This work has been supported by Ministry of Education and Science of Ukraine within project 24БФ051-01 "Synthesis of biocompatible metal-ceramic composites to improve the wear resistance of medical instruments and titanium-based implants".

REFERENCES

1. B. Cantor, I.T.H. Chang, P. Knight, A.J.B. Vincent, *Mater. Sci. Eng.* **213**, 375 (2004).
2. Y. Zhang, T.T. Zuo, Z. Tang, M.C. et al., *Prog. Mater. Sci.* **61**, 1 (2014).
3. C.M. Rost, E. Sachet, T. Borman, et al., *Nat. Commun.* **6**, 8485 (2015).
4. B.L. Music, D. Gilbert, T. Zac Ward, et al., *APL Mater.* **8**, 040912 (2020).
5. A. Sarkar, Q. Wang, A. Schiele, et al., *Adv. Mater.* **31**, 1806236 (2019).
6. A.K. Berardan, S. Meena, C. Franger, et al., *J. Alloy. Compd.* **704**, 693 (2017).
7. W. Hong, F. Chen, Q. Shen, et al., *J. Am. Ceram. Soc.* **102**, No 4, 2228 (2019).
8. J. Rodriguez-Carvajal, *Phys. B* **192**, 55 (1993).
9. A. Le Bail, H. Duroy, J.L. Fourquet, *Mat. Res. Bull.* **23**, 447 (1988).
10. R.D. Shannon, *Acta Cryst.* **A32**, 751 (1976).
11. J. Malek, J. Sestak, F. Rouquerol, et al., *J. Thermal. Anal.* **38**, 71 (1992).
12. F. Liu, F. Sommer, C. Bos, E. J. Mittemeijer, *Int. Mater. Rev.* **52**, 193 (2007).
13. M.I. Daoudi, A. Triki, A. Redjaimia, *J. Thermal. Anal. Calorim.* **104**, 627 (2011).

Деякі кінетичні особливості формування високоентропійного оксиду $Co_{0.2}Ni_{0.2}Cu_{0.2}Mg_{0.2}Zn_{0.2}O$

М.П. Семенько

Київський національний університет імені Тараса Шевченка, 01601 Київ, Україна

Методами рентгенівської дифракції вперше досліджено кінетику формування високоентропійного оксиду $Co_{0.2}Ni_{0.2}Cu_{0.2}Mg_{0.2}Zn_{0.2}O$ із вихідної порошкової суміші оксидних складових. Показано, що розчинення оксиду CuO на останньому етапі формування цього оксиду може бути описаний з використанням моделі Мелла-Джонсона-Аврамі. На основі аналізу результатів, отриманих в ізотермічних умовах, оцінено кінетичні параметри процесу. Значення показника Аврамі свідчить, що процес формування на цьому етапі відбувається без утворення зародків нової фази за дифузійним механізмом зі зміною характеру дифузії при наближенні складу до номінального.

Ключові слова: Високо-ентропійний оксид, Кінетичний параметр, Рентгенівська дифракція.